

Steric Protection of a Photosensitizer in a *N,N*-Bis[2-(2-pyridyl)ethyl]-2-phenylethylamine-copper(II) Bowl that Enhances Red Light-Induced DNA Cleavage Activity

Shanta Dhar, Munirathinam Nethaji, and Akhil R. Chakravarty*

Department of Inorganic & Physical Chemistry, Indian Institute of Science, Bangalore 560012, India

Received April 6, 2005

Ternary copper(II) complexes [Cu(py₂phe)B](ClO₄)₂ (**1–3**), where py₂phe is a tripodal ligand *N,N*-bis[2-(2-pyridyl)ethyl]-2-phenylethylamine and B is a heterocyclic base (viz., 1,10-phenanthroline (phen, **1**), dipyrido[3,2-d:2',3'-f]-quinoxaline (dpq, **2**), or dipyrido[3,2-a:2',3'-c]phenazine (dppz, **3**)), are prepared and their DNA-binding and photoinduced DNA-cleavage activities are studied. Complex **1** has been structurally characterized by single crystal X-ray crystallography. The molecular structure shows an axially elongated square-pyramidal (4 + 1) coordination geometry in which the phen ligand binds at the basal plane. The tripodal ligand py₂phe displays an axial–equatorial binding mode with the amine nitrogen bonded at the axial site. A chemically significant CH– π interaction involving the CH moiety of the phenyl group of the tripodal ligand and the aromatic ring of phen is observed. The complexes display good binding propensity to calf thymus DNA giving a relative order of **3** (dppz) > **2** (dpq) > **1** (phen). The DNA binding constants (K_b) for **1–3**, determined from absorption spectral studies, are 6.2×10^3 , 1.0×10^4 , and 5.7×10^4 M⁻¹, respectively. The complexes show chemical nuclease activity in the presence of 3-mercaptopropionic acid as a reducing agent forming hydroxyl radicals as the cleavage active species. The photoinduced DNA-cleavage activity of the complexes has been studied using UV radiation of 365 nm and red light of 632.8 and 694 nm. The phen complex in absence of any photosensitizing moiety does not show any DNA cleavage upon photoirradiation. The dpq and dppz ligands with their photoactive quinoxaline and phenazine moieties display significant photoinduced DNA-cleavage activity. The dppz complex is more active than its dpq analogue because of the better steric protection of the DNA-bound photosensitizing dppz ligand from the solvent molecules. Control experiments reveal the formation of singlet oxygen in the light-induced DNA-cleavage reactions. The observed efficient photoinduced DNA-cleavage activity of **2** and **3** is akin to the “light switch” effect known for the tris-chelates of ruthenium(II).

Introduction

Transition metal complexes with the ability to bind and cleave DNA under physiological conditions are of interest because of their varied uses in nucleic acid chemistry.^{1–9} Among several notable developments in this area of chemistry, the molecular “light switch” effect, in which octahedral

2,2'-bipyridine (bpy) and 1,10-phenanthroline (phen) complexes of ruthenium and rhodium with dipyrido[3,2-a:2',3'-c]phenazine (dppz) bases and extended planar aromatic heterocyclic rings show significant enhancement of emission

* To whom correspondence should be addressed. E-mail: arc@ipc.iisc.ernet.in.

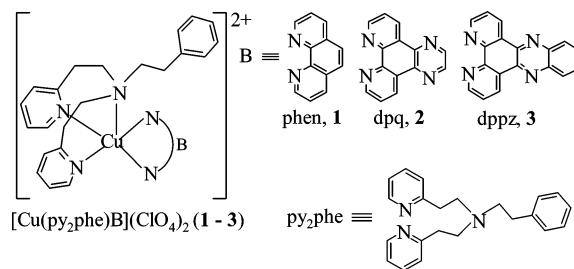
- (1) Erkkila, K. E.; Odom, D. T.; Barton, J. K. *Chem. Rev.* **1999**, *99*, 2777.
- (2) (a) Sigman, D. S.; Mazumder, A.; Perrin, D. M. *Chem. Rev.* **1993**, *93*, 2295. (b) Sigman, D. S. *Acc. Chem. Res.* **1986**, *19*, 180.
- (3) (a) Meunier, B. *Chem. Rev.* **1992**, *92*, 1411. (b) Pratiel, G.; Bernadou, J.; Meunier, B. *Adv. Inorg. Chem.* **1998**, *45*, 251.
- (4) Chifotides, H. T.; Dunbar, K. R. *Acc. Chem. Res.* **2005**, *38*, 146.
- (5) (a) Jamieson, E. R.; Lippard, S. J. *Chem. Rev.* **1999**, *99*, 2467. (b) Lippard, S. J.; Berg, J. M. *Principles of Bioinorganic Chemistry*; University Science Books: Mill Valley, CA, 1994.

- (6) (a) Reedijk, J. *J. Inorg. Biochem.* **2001**, *86*, 89. (b) Hegg, E. L.; Burstyn, J. N. *Coord. Chem. Rev.* **1998**, *173*, 133. (c) Cowan, J. A. *Chem. Rev.* **1998**, *98*, 1067. (d) Sreedhara, A.; Cowan, J. A. *J. Biol. Inorg. Chem.* **2001**, *6*, 337. (e) Wolkenberg, S. E.; Boger, D. L. *Chem. Rev.* **2002**, *102*, 2477.
- (7) (a) Szacilowski, K.; Macyk, W.; Drzewiecka-Matuszek, A.; Brindell, M.; Stochel, G. *Chem. Rev.* **2005**, *105*, 2647. (b) Armitage, B. *Chem. Rev.* **1998**, *98*, 1171. (c) McMillin, D. R.; McNett, K. M. *Chem. Rev.* **1998**, *98*, 1201. (c) Metcalfe, C.; Thomas, J. A. *Chem. Soc. Rev.* **2003**, *32*, 215.
- (8) Burrows, C. J.; Muller, J. G. *Chem. Rev.* **1998**, *98*, 1109.
- (9) (a) Pogozelski, W. K.; Tullius, T. D. *Chem. Rev.* **1998**, *98*, 1089. (b) Lang, K.; Mosinger, J.; Wagnerova, D. M. *Coord. Chem. Rev.* **2004**, *248*, 321.

intensity upon intercalative binding to duplex DNA, has made such complexes suitable as photophysical probes in DNA conformational studies.^{1,10–16} Steric protection of the photosensitizer in a DNA-bound form is known to increase its excited-state lifetime.¹⁶ Such a phenomenon could be of use in designing non-porphyrinic transition metal complexes for photoinduced DNA-cleavage studies by selective choice of ancillary ligands that could protect the photosensitizer from solvent interactions and enhance the generation of cytotoxic singlet oxygen for oxidative cleavage of DNA. We recently reported the effect of steric protection of the photosensitizer in significantly augmenting the photoinduced DNA-cleavage activity of ternary copper(II) scorpionates $[\text{Cu}(\text{Tp}^{\text{Ph}})\text{B}](\text{ClO}_4)$ in which the sterically demanding tripodal ligand tris-(3-phenylpyrazolyl)borate (HTp^{Ph}) in a $\{\text{Cu}(\text{Tp}^{\text{Ph}})\}$ bowl effectively encloses the photosensitizer, like dppz (B).¹⁷ Our observation is akin to the molecular light switch effect exhibited by the tris-chelates of ruthenium(II).

With an aim to explore this steric effect further, we have chosen a tripodal ligand derived from 2-vinylpyridine and phenylethylamine. This ligand has a pendant phenylethyl arm that is expected to increase the binding propensity of the complex to duplex DNA by noncovalent hydrophobic interactions in addition to shielding the photosensitizer in its photoexcited triplet electronic state from quenching by the solvent water molecules. We have chosen dipyridoquinoxaline (dpq) and dipyridophenazine (dppz) bases as photosensitizers because their copper(II) complexes are known to exhibit visible light-induced DNA-cleavage activity involving the photoexcited $^3(n-\pi^*)$ and $^3(\pi-\pi^*)$ states of the quinoxaline and phenazine moieties, respectively.^{18,19} Besides, the copper(II) complexes exhibiting metal-assisted red light-induced DNA-cleavage activity have potential for application in the chemistry of photodynamic therapy (PDT).^{20–25} One of the basic requirements of a photosensi-

Scheme 1. Ternary Structures of the Copper(II) Complexes 1–3 and the Phenanthroline Bases Used



tizer with a significantly high molar-extinction coefficient to be effective as a drug in PDT is the photoactivation in the “phototherapeutic window” of ca. 620 to 850 nm. The PDT drug Photofrin is a porphyrin-based compound that causes DNA damage at 630 nm. Synthesis of non-porphyrinic copper compounds showing light-induced DNA cleavage activity in this “phototherapeutic window” is our objective. Our previous reports have shown that copper(II) complexes efficiently cleave DNA on photoexposure to red light involving the d–d and charge-transfer bands in the photoexcitation process.^{18,26} Using a tripodal ligand, *N,N*-bis[2-(2-pyridyl)ethyl]-2-phenylethylamine (py₂phe), we were able to synthesize new ternary copper(II) complexes $[\text{Cu}(\text{py}_2\text{phe})\text{B}](\text{ClO}_4)_2$ (1–3) that exhibit a visible band at a significantly longer wavelength than the ternary copper(II) scorpionates [B = phen (1), dipyrido[3,2-d:2',3'-f]quinoxaline (dpq, 2), dppz (3); Scheme 1].¹⁷ Interestingly, the visible band of 3 at 701 nm is at a longer wavelength than the visible bands generally observed for porphyrins.^{27,28} Herein, we report the synthesis, DNA binding and red light-induced DNA-cleavage activity of 1–3. The phen complex has been structurally characterized by X-ray crystallography. The significant result of this study is the efficient photoinduced DNA-cleavage activity of the dppz complex at 694 nm using a pulsed ruby laser. The importance of steric protection of the photosensitizer in enhancing the cleavage activity of the ternary copper(II) complexes is observed.

Experimental Section

Materials and Measurements. All reagents and chemicals were procured from commercial sources and used without further purification. Solvents used were purified by standard procedures.²⁹ Calf thymus DNA and supercoiled pUC19 DNA (cesium chloride purified) were purchased from Bangalore Genie (India). Agarose

- (10) (a) Friedman, A. E.; Chambron, J.-C.; Sauvage, J.-P.; Turro, N. J.; Barton, J. K. *J. Am. Chem. Soc.* **1990**, *112*, 4960. (b) Hartshorn, R. M.; Barton, J. K. *J. Am. Chem. Soc.* **1992**, *114*, 5919. (c) Dupureur, C. M.; Barton, J. K. *J. Am. Chem. Soc.* **1994**, *116*, 10286. (d) Turro, C.; Bossmann, S. H.; Jenkins, Y.; Barton, J. K.; Turro, N. J. *J. Am. Chem. Soc.* **1995**, *117*, 9026. (e) Ruba, E.; Hart, J. R.; Barton, J. K. *Inorg. Chem.* **2004**, *43*, 4570.
- (11) Gupta, N.; Grover, N.; Neyhart, G. A.; Liang, W.; Singh, P.; Thorp, H. H. *Angew. Chem., Int. Ed. Engl.* **1992**, *31*, 1048.
- (12) (a) Hiort, C.; Lincoln, P.; Norden, B. *J. Am. Chem. Soc.* **1993**, *115*, 3448. (b) Metcalfe, C.; Adams, H.; Haq, I.; Thomas, J. A. *Chem. Commun.* **2003**, 1152.
- (13) (a) Arounaguirri, S.; Maiya, B. G. *Inorg. Chem.* **1999**, *38*, 842. (b) Arounaguiry, A.; Maiya, B. G. *Inorg. Chem.* **2000**, *39*, 4246.
- (14) Liu, Y.; Chouai, A.; Degtyareva, N. N.; Lutterman, D. A.; Dunbar, K. R.; Turro, C. J. *Am. Chem. Soc.* **2005**, *127*, 10796.
- (15) Che, C.-M.; Yang, M.; Wong, K.-H.; Chan, H.-L.; Lam, W. *Chem.—Eur. J.* **1999**, *5*, 3350.
- (16) Olson, E. J. C.; Hu, D.; Hormann, A.; Jonkman, A. M.; Arkin, M. R.; Stemp, E. D. A.; Barton, J. K.; Barbara, P. F. *J. Am. Chem. Soc.* **1997**, *119*, 11458.
- (17) Dhar, S.; Chakravarty, A. R. *Inorg. Chem.* **2005**, *44*, 2582.
- (18) Dhar, S.; Senapati, D.; Reddy, P. A. N.; Das, P. K.; Chakravarty, A. R. *Chem. Commun.* **2003**, 2452.
- (19) Gupta, T.; Dhar, S.; Nethaji, M.; Chakravarty, A. R. *Dalton Trans.* **2004**, 1896.
- (20) Clarke, M. J. *Coord. Chem. Rev.* **2003**, *236*, 209.
- (21) Henderson, B. W.; Busch, T. M.; Vaughan, L. A.; Frawley, N. P.; Babich, D.; Sisa, T. A.; Zollo, J. D.; Dee, A. S.; Cooper, M. T.; Bellnier, D. A.; Greco, W. R.; Oseroff, A. R. *Cancer Res.* **2000**, *60*, 525.

- (22) De Rosa, M. C.; Crutchley, R. J. *Coord. Chem. Rev.* **2002**, *233–234*, 351.
- (23) Ali, H.; van Lier, J. E. *Chem. Rev.* **1999**, *99*, 2379.
- (24) (a) Dougherty, T. J.; Gomer, C. J.; Henderson, B. W.; Jori, G.; Kessel, D.; Korbelik, M.; Moan, J.; Peng, Q. *J. Natl. Cancer Inst.* **1998**, *90*, 889. (b) Sessler, J. L.; Hemmi, G.; Mody, T. D.; Murai, T.; Burrell, A.; Young, S. W. *Acc. Chem. Res.* **1994**, *27*, 43.
- (25) Sternberg, E. D.; Dolphin, D.; Brückner, C. *Tetrahedron* **1998**, *54*, 4151.
- (26) Dhar, S.; Senapati, D.; Das, P. K.; Chattopadhyay, P.; Nethaji, M.; Chakravarty, A. R. *J. Am. Chem. Soc.* **2003**, *125*, 12118.
- (27) Bonnett, R.; Martinez, G. *Tetrahedron* **2001**, *57*, 9513.
- (28) (a) Berenbaum, M. C.; Bonnett, R.; Scourides, P. A. *Br. J. Cancer* **1982**, *45*, 571. (b) Bonnett, R.; Berenbaum, M. C. *Adv. Exp. Med. Biol.* **1983**, *160*, 241.
- (29) Perrin, D. D.; Armarego, W. L. F.; Perrin, D. R. *Purification of Laboratory Chemicals*; Pergamon Press: Oxford, U.K., 1980.

(molecular biology grade) and ethidium bromide (EB) were from Sigma (USA). 2-Vinylpyridine and phenylethylamine were from Aldrich (USA). Ligands py_2phe , dpq , and dppz were prepared using literature procedures.³⁰ Tris-HCl buffer solution was prepared using deionized sonicated triple-distilled water.

The elemental analyses were done using a Thermo Finnigan Flash EA 1112 CHNSO analyzer. The infrared, electronic, and fluorescence spectral data were obtained using Perkin-Elmer Spectrum One FT-IR, Perkin-Elmer Lambda 35 UV-vis, and Perkin-Elmer LS-50B spectrophotometers, respectively. Electrochemical measurements were done at 25 °C on an EG & G PAR model 253 Versa Stat potentiostat/galvanostat with electrochemical analysis software 270 for cyclic voltammetric work using a three electrode setup consisting of glassy carbon working, platinum wire auxiliary, and saturated calomel reference electrode. Magnetic susceptibility data at 298 K were obtained for the polycrystalline samples using George Associates Inc. Lewis-coil-force magnetometer system (Berkeley, CA).

Preparation of $[\text{Cu}(\text{py}_2\text{phe})(\text{phen})](\text{ClO}_4)_2$ (1) and $[\text{Cu}(\text{py}_2\text{phe})(\text{dpq})](\text{ClO}_4)_2$ (2). Complexes **1** and **2** were prepared by a general procedure in which $\text{Cu}(\text{ClO}_4)_2 \cdot 6\text{H}_2\text{O}$ (370 mg, 1.0 mmol) was reacted with the tripodal ligand py_2phe (400 mg, 1.2 mmol) and the corresponding base [0.9 mmol; phen, 180 mg; dpq, 210 mg] in 15 mL of acetonitrile. The solution was stirred for 5 h at 25 °C. The product was obtained as a solid in an ~70% yield upon the addition of diethyl ether to the reaction mixture. The solid was isolated, washed with diethyl ether, and dried in a vacuum over P_4O_{10} . The complexes were crystallized by a diffusion technique in which diethyl ether was layered on the top of the acetonitrile solution of the complexes. Anal. Calcd for $\text{C}_{34}\text{H}_{33}\text{CuN}_5\text{O}_8\text{Cl}_2$ (**1**): C, 52.75; H, 4.27; N, 9.05. Found: C, 53.09; H, 3.95; N, 9.25. FT-IR (KBr phase): 3435br, 1615m, 1525w, 1492w, 1422m, 1312w, 1092vs, 852m, 769m, 713m, 699w, 619s, 426w cm^{-1} (br, broad; vs, very strong; s, strong; m, medium; w, weak). UV-vis in DMF, λ_{max} (ϵ): 273 (26400), 442 (550), 675 nm ($110 \text{ M}^{-1} \text{ cm}^{-1}$). Magnetic data [μ_{eff} at 298 K]: 1.78 μ_{B} . Anal. Calcd for $\text{C}_{36}\text{H}_{33}\text{CuN}_7\text{O}_8\text{Cl}_2$ (**2**): C, 52.33; H, 3.99; N, 11.87. Found: C, 52.38; H, 4.08; N, 12.03. FT-IR (KBr phase): 3443br, 1615m, 1587m, 1539w, 1488s, 1438w, 1409s, 1383s, 1311w, 1220w, 1095vs, 814m, 766w, 738m, 618s, 428w cm^{-1} . UV-vis in DMF, λ_{max} (ϵ): 267 (47000), 336 (8000), 448 (2200), 683 nm ($97 \text{ M}^{-1} \text{ cm}^{-1}$). Magnetic data [μ_{eff} at 298 K]: 1.92 μ_{B} .

Preparation of $[\text{Cu}(\text{py}_2\text{phe})(\text{dppz})](\text{ClO}_4)_2$ (3). Complex **3** was prepared by reacting $\text{Cu}(\text{ClO}_4)_2 \cdot 6\text{H}_2\text{O}$ (370 mg, 1.0 mmol) with the tridentate ligand py_2phe (1.2 mmol, 400 mg) and dppz base (0.9 mmol, 260 mg) in 15 mL of methanol. The solution was stirred for 5 h at 25 °C. The product was obtained as a solid in an ~65% yield upon addition of diethyl ether to the reaction mixture. The product was isolated, washed with diethyl ether, and dried in a vacuum over P_4O_{10} . The complex was crystallized by a method similar to that described for complexes **1** and **2**. Anal. Calcd for $\text{C}_{40}\text{H}_{35}\text{CuN}_7\text{O}_8\text{Cl}_2$ (**3**): C, 54.83; H, 3.99; N, 11.17. Found: C, 54.77; H, 3.83; N, 11.35. FT-IR (KBr phase): 3447br, 1608m, 1532w, 1495s, 1430m, 1359m, 1229s, 1092vs, 816w, 769m, 729m, 619s, 426m cm^{-1} . UV-vis in DMF, λ_{max} (ϵ): 273 (11600), 367 (4500), 701 nm ($78 \text{ M}^{-1} \text{ cm}^{-1}$). Magnetic data [μ_{eff} at 298 K]: 1.85

Table 1. Selected Crystallographic Data for $[\text{Cu}(\text{py}_2\text{phe})(\text{phen})](\text{ClO}_4)_2 \cdot \text{MeCN}$ (**1**·MeCN)

chemical formula	$\text{C}_{36}\text{H}_{36}\text{Cl}_2\text{CuN}_6\text{O}_8$
fw (g mol ⁻¹)	815.15
space group	$P2_1/c$
<i>a</i> (Å)	9.5591(14)
<i>b</i> (Å)	27.757(4)
<i>c</i> (Å)	14.372(2)
β (deg)	100.484(2)
<i>V</i> (Å ³)	3749.7(10)
<i>Z</i>	4
<i>T</i> (K)	293(2)
ρ_{calcd} (g cm ⁻³)	1.444
λ (Mo K α) (Å)	0.71073
μ (cm ⁻¹)	7.84
<i>R1</i> (F_o) ^a [R all data]	0.0559 [0.0663]
wR2 (F_o) ^b [wR2 (all data)]	0.1517 [0.1608]

^a $R1 = \sum ||F_o| - |F_c|| / \sum |F_o|$. ^b $wR2 = [\sum w(|F_o| - |F_c|)^2 / \sum w |F_o|^2]^{1/2}$, where $w = 1/[\sigma^2(F_o^2) + (AP)^2 + BP]$ where $\sigma = [\max(F_o^2, 0) + 2F_c^2]/3$. *A* and *B* values are 0.0896 and 4.4947, respectively.

μ_{B} . The complexes were soluble in acetonitrile and dimethylformamide, moderately soluble in methanol, and sparingly soluble in water.

X-ray Crystallographic Procedures. Single crystals of the phen complex as **1**·MeCN were grown by a diffusion technique in which diethyl ether was layered on the top of an acetonitrile solution of the complex. A crystal of 0.23 × 0.19 × 0.15 mm was mounted on a glass fiber using epoxy cement. The X-ray diffraction data were measured in frames with increasing ω (width of 0.3° per frame) at a scan speed of 8 s per frame using a Bruker SMART APEX CCD diffractometer, equipped with a fine-focus sealed-tube Mo K α X-ray source. SMART was used for data acquisition, and SAINT was used for data extraction. Empirical absorption corrections were made on the intensity data.³¹ The structure was solved and refined using the SHELX system of programs.³² There was one lattice MeCN molecule in the crystallographic asymmetric unit. All non-hydrogen atoms except the solvent MeCN molecule were refined anisotropically. The hydrogen atoms belonging to the complex were located from the difference Fourier map and refined isotropically. The perchlorate anions showed positional disorder. For the oxygen atoms bonded to Cl(1), only one oxygen atom (viz., O(2)) was refined with a site-occupancy factor (SOF) of 1.0. There were two peaks for the O(1) atom with SOF values of 0.6 and 0.4, two peaks for O(3) with SOF values of 0.7 and 0.3, and two peaks for O(4) with SOF values of 0.6 and 0.4. For the other perchlorate anion, while the oxygen atoms O(5), O(6), and O(8) were refined well, each with a SOF of 1.0, atom O(7) was found to be disordered to two sites that were refined with an SOF value of 0.5. The structure was refined with a goodness-of-fit (GOF) value of 1.037. The maximum shift/esd value and the highest peak in the final difference Fourier map were 0.001 and 0.894 e Å⁻³, respectively. Selected crystallographic data are given in Table 1. The perspective view of the cationic complex was obtained using the ORTEP program.³³

DNA Binding and Cleavage Experiments. The relative binding of the complexes to calf thymus (CT) DNA was studied using the fluorescence spectral method with an ethidium bromide-bound (EB-bound) CT DNA solution in Tris-HCl/NaCl buffer (pH, 7.2). The concentration of CT DNA was determined from its absorption intensity at 260 nm with a molar extinction coefficient of 6600

(30) Karlin, K. D.; Hayes, J. C.; Gultneh, Y.; Cruse, R. W.; McKown, J. W.; Hutchinson, J. P.; Zubieta, J. *J. Am. Chem. Soc.* **1984**, *106*, 2121. (b) Dickeson, J. E.; Summers, L. A. *Aust. J. Chem.* **1970**, *23*, 1023. (c) Amouyal, E.; Homsí, A.; Chambron, J.-C.; Sauvage, J.-P. *J. Chem. Soc., Dalton Trans.* **1990**, 1841.

(31) Walker, N.; Stuart, D. *Acta Crystallogr. A* **1993**, *39*, 158.

(32) Sheldrick, G. M. *SHELX-97, Programs for Crystal Structure Solution and Refinement*; University of Göttingen: Göttingen, Germany, 1997.

(33) Johnson, C. K. *ORTEP*, Report ORNL-5138; Oak Ridge National Laboratory: Oak Ridge, TN, 1976.

$M^{-1} cm^{-1}$.³⁴ Fluorescence intensities at 601 nm (510 nm excitation) were measured at different complex concentrations. Addition of the complex showed a reduction in the emission intensity. The relative binding propensity of the complexes to CT DNA was determined from the comparison of the slopes of the lines in the fluorescence intensity versus complex concentration plot.³⁵ The apparent binding constant (K_{app}) was calculated from the equation $K_{EB}[EB] = K_{app}[\text{complex}]$, where the complex concentration was the value at a 50% reduction of the fluorescence intensity of EB and $K_{EB} = 1.0 \times 10^7 M^{-1}$ ($[EB] = 1.3 \mu M$). DNA-melting experiments were carried out by monitoring the absorbance (260 nm) of CT-DNA (150 μM NP) at various temperatures in the absence and presence of the complexes at a 2:1 ratio (DNA/complex) using a Peltier system attached to a UV-vis spectrophotometer. The phosphate buffer (pH 6.85) solution containing the ternary complex and CT DNA was stirred, and the temperature was elevated gradually from 40 to 95 °C at a rate of 1.0 °C per 4 min. The absorption spectral titration method was used to determine the binding constants (K_b) of the complexes using the expression $[DNA]/(\epsilon_a - \epsilon_f) = [DNA]/(\epsilon_b - \epsilon_f) + 1/K_b(\epsilon_b - \epsilon_f)$, where ϵ_a , ϵ_f , and ϵ_b are the apparent absorption coefficient, the ϵ of the complex in free form, and the ϵ of the complex in the fully bound form, respectively. The K_b value was obtained from the $[DNA]/(\epsilon_a - \epsilon_f)$ versus $[DNA]$ plot.³⁶

Photoinduced cleavage of supercoiled (SC) pUC19 DNA by the complexes was studied by agarose gel electrophoresis. The reactions were carried out under illuminated conditions using a UV lamp of 365 nm (12 W, sample area of illumination 45 mm²), a 632.8 nm CW He-Ne laser (3 mW, beamsize 2 mm, Scientifica-Cook Ltd make, U.K.), and a 694 nm pulsed ruby laser (30 mJ/P peak power, Lumonics make, 1/6 Hz, 20 ns, beam width of 1 mm). Eppendorf and glass vials were used for the UV and visible light experiments, respectively, in a dark room at 25 °C using SC DNA (1 μL , 0.2 μg , 33 μM) in 50 mM tris-(hydroxymethyl)methane-HCl (Tris-HCl) buffer (pH 7.2, ionic strength 25 mM) containing 50 mM NaCl and the complex (varied concentrations). The solution path length used for illumination in the sample vial was 6 mm. After photoexposure, the sample was incubated for 1 h at 37 °C, followed by the addition to the loading buffer containing 25% bromophenol blue, 0.25% xylene cyanol, and 30% glycerol (3 μL), and the solution was finally loaded on an 0.8% agarose gel containing 1.0 $\mu g/mL$ ethidium bromide. Electrophoresis was carried out in a dark chamber for 3 h at 40 V in TAE (Tris-acetate-EDTA) buffer. Bands were visualized by UV light and photographed. The extent of cleavage of the SC DNA was determined by measuring the intensities of the bands using a UVITEC Gel Documentation System. Corrections were made to the data for the low level of nicked-circular (NC) form present in the original SC DNA sample and for the low affinity of EB binding to SC compared to the NC form of DNA.³⁷ Experiments were carried out in the presence of different additives for mechanistic investigations. These reactions were carried out by adding reagents to SC DNA prior to the addition of the complex before photoirradiation. The "chemical nuclease" activity of the complexes was studied using 3-mercaptopropionic acid (MPA) as a reducing agent under dark reaction conditions. Supercoiled pUC19 DNA (0.2 μg , 33 μM) in 50 mM Tris-HCl buffer (pH 7.2) containing 50 mM NaCl was treated with the metal

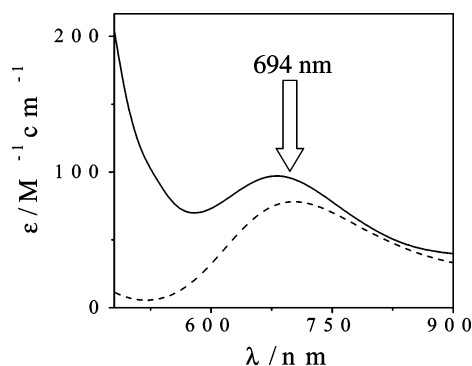


Figure 1. d-d band in the electronic spectra of $[Cu(py_2phe)(dpq)](ClO_4)_2$ (**2**, —) and $[Cu(py_2phe)(dppz)](ClO_4)_2$ (**3**, ---) in DMF.

complex (40 μM) and MPA (5 mM), followed by dilution with the Tris-HCl buffer to a total volume of 18 μL . The samples were incubated for 1 h at 37 °C in the dark. The concentrations of the complexes or the additives corresponded to the quantity of the sample in 2 μL stock solution used prior to dilution to the 18 μL final volume with Tris-HCl buffer.

Results and Discussion

Synthesis and Structural Aspects. Ternary copper(II) complexes $[Cu(py_2phe)B](ClO_4)_2$ ($B = \text{phen}$, **1**; dpq , **2**; $dppz$, **3**) with the py_2phe tripodal ligand and a bidentate phenanthroline base (B) are prepared in high yield and characterized from analytical and spectral data. The one-electron paramagnetic complexes exhibit a d-d band in the range of 675 to 701 nm in DMF (Figure 1). The analogous {tris(3-phenylpyrazolyl)borate}copper(II) ternary complexes are known to show the d-d band near 650 nm.³⁸ Complexes **1–3** show a characteristic infrared band for the anionic perchlorate at $\sim 1090 cm^{-1}$. The redox active complexes display one-electron quasi-reversible cyclic voltammetric responses assignable to the Cu(II)/Cu(I) couple at -0.016 , 0.017 , and 0.058 V vs SCE for **1–3** in DMF-Tris-HCl buffer medium giving peak-to-peak separations (ΔE_p) of 230, 220, and 190 mV, respectively, at a scan rate of $50 mV s^{-1}$. The $E_{1/2}$ values show greater stabilization of the copper(I) state in the $dppz$ complex resulting from the higher π acidity of the ligand in the presence of an extended aromatic phenazine moiety.

The phen complex **1**·MeCN is structurally characterized by single-crystal X-ray diffraction technique. A perspective view of the cationic complex is shown in Figure 2, and selected bond distances and bond angles data are presented in Table 2. The crystal structure of the complex consists of a discrete monomeric copper(II) species with two perchlorate anions and one lattice MeCN molecule in the crystallographic asymmetric unit belonging to monoclinic space group $P2_1/c$. The geometry of the copper atom is distorted square pyramidal ($\tau = 0.35$) with a CuN_5 coordination in which the phen ligand occupies the basal plane.³⁹ The tripodal ligand shows axial-equatorial bonding modes. The amine nitrogen atom N(1) binds at the elongated axial site giving

(34) Reichmann, M. E.; Rice, S. A.; Thomas, C. A.; Doty, P. *J. Am. Chem. Soc.* **1954**, *76*, 3047.

(35) Lee, M.; Rhodes, A. L.; Wyatt, M. D.; Forrow, S.; Hartley, J. A. *Biochemistry* **1993**, *28*, 7268.

(36) Wolf, A.; Shimer, G. H., Jr.; Meehan, T. *Biochemistry* **1987**, *26*, 6392.

(37) Bernadou, J.; Pratiel, G.; Bennis, F.; Girardet, M.; Meunier, B. *Biochemistry* **1989**, *28*, 7268.

(38) Dhar, S.; Reddy, P. A. N.; Nethaji, M.; Mahadevan, S.; Saha, M. K.; Chakravarty, A. R. *Inorg. Chem.* **2002**, *41*, 3469.

(39) Addison, A. W.; Rao, T. N.; Reedijk, J.; Rijn, J. V.; Verschoor, G. C. *J. Chem. Soc., Dalton Trans.* **1984**, 1349.

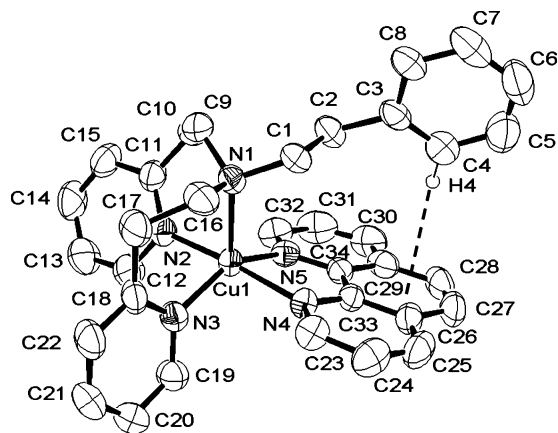


Figure 2. ORTEP view of the cationic complex in $[\text{Cu}(\text{py}_2\text{phe})(\text{phen})](\text{ClO}_4)_2 \cdot \text{MeCN}$ (**1**·MeCN) showing thermal ellipsoids at the 50% probability level and the atom numbering scheme. The CH– π interaction is also shown (---).

Table 2. Selected Bond Distances (Å) and Angles (deg) for $[\text{Cu}(\text{py}_2\text{phe})(\text{phen})](\text{ClO}_4)_2 \cdot \text{MeCN}$ (**1**·MeCN)

Cu(1)–N(1)	2.253(3)
Cu(1)–N(2)	2.004(3)
Cu(1)–N(3)	2.037(3)
Cu(1)–N(4)	2.027(3)
Cu(1)–N(5)	2.044(3)
N(2)–Cu(1)–N(4)	170.61(12)
N(2)–Cu(1)–N(3)	91.34(13)
N(4)–Cu(1)–N(3)	90.32(12)
N(2)–Cu(1)–N(5)	92.96(13)
N(4)–Cu(1)–N(5)	80.97(11)
N(3)–Cu(1)–N(5)	149.28(12)
N(2)–Cu(1)–N(1)	92.94(12)
N(4)–Cu(1)–N(1)	95.98(11)
N(3)–Cu(1)–N(1)	98.05(12)
N(5)–Cu(1)–N(1)	112.07(11)

a Cu(1)–N(1) distance of 2.253(3) Å. The average Cu(1)–N(basal plane) distance is 2.027[3] Å. The phenyl group of the tripodal ligand py_2phe is involved in a moderately strong CH– π interaction with the aromatic ring of the phen ligand giving a H(4)···C_o^{phen} distance of 2.667 Å and a C(4)–H(4)···C_o^{phen} angle of 140.42°, where C_o^{phen} is the centroid of the phen ligand.

DNA Binding Properties. The mode and propensity of binding of the complexes to calf thymus (CT) DNA are studied by different techniques. The fluorescence spectral method is used to study the relative binding of these complexes to CT DNA. The emission intensity of ethidium bromide (EB) is used as a spectral probe as EB shows reduced emission intensity in buffer because of quenching by the solvent molecules and a significant enhancement of the intensity when bound to DNA. Binding of the complexes to DNA decreases the emission intensity and the extent of the reduction of the emission intensity gives a measure of the DNA binding propensity of the complexes. The apparent binding constant (K_{app}) values for **1–3** are 1.0×10^5 , 5.7×10^5 , and $2.0 \times 10^6 \text{ M}^{-1}$, respectively. The significantly high K_{app} value for the dppz complex, in comparison to that of its phen analogue, could be the result of the presence of its extended aromatic rings which facilitate its DNA binding propensity. The binding data can be compared with those of the analogous copper(II) scorpionates $[\text{Cu}(\text{Tp}^{\text{Ph}})\text{B}](\text{ClO}_4)_2$,

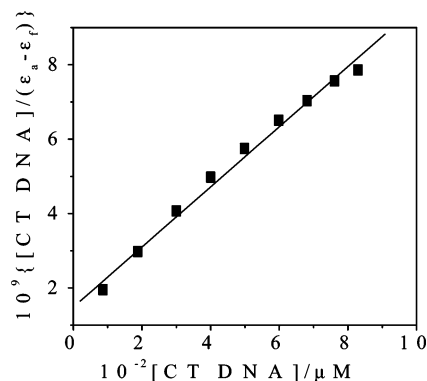


Figure 3. Plot of $[\text{DNA}]/(\epsilon_a - \epsilon_f)$ vs $[\text{DNA}]$ for **3** using absorption spectral data.

where B is the heterocyclic base like phen, dpq, or dppz and Tp^{Ph} is monoanionic tris(3-phenylpyrazolyl)borate.³⁸ The scorpionates, which have the metal-bound DNA-binder heterocyclic base in the $\{\text{Cu}^{\text{II}}(\text{Tp}^{\text{Ph}})\}$ bowl, do not show any significant DNA binding because of the steric encumbrance of the tripodal ligand. The efficient DNA binding of complexes **1–3** could be the result of the less steric bulk of the py_2phe tripodal ligand, the greater positive charge of the complex, and the possible favorable hydrophobic interactions of the pendant phenyl group of py_2phe with the DNA. The reduction of the emission intensity of EB upon increasing the complex concentration could be caused by the displacement of the DNA-bound EB by the copper(II) complex or the result of quenching of the EB fluorescence, resulting from the binding of the one-electron paramagnetic copper(II) complex to DNA.

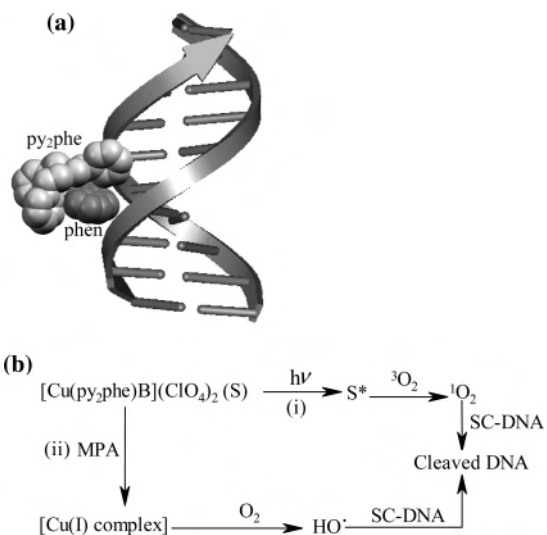
The binding of complexes **1–3** to CT DNA has been studied from the thermal denaturation profile of the DNA. We observed a minor increase in the melting temperature (T_m) on addition of the complex to CT DNA. The ΔT_m values for **1–3** are 4.0, 5.5, and 7.2 °C, respectively, in which the free CT DNA gives a T_m value of 71 °C. The results primarily suggest the groove-binding nature of the complexes. We also carried out absorption spectral measurements to determine the binding constants of the complexes to CT DNA by monitoring the change of the intensity of the spectral bands at 273 nm for **1**, 336 nm for **2**, and 367 nm for **3** with increasing concentration of CT DNA. An intercalative mode of binding generally gives hypochromism along with a red shift (bathochromic shift) of the electronic spectral band.⁴⁰ The extent of the hypochromism gives a measure of the strength of the intercalative binding/interaction. The phen complex, **1**, was found to show a minor bathochromic shift of ca. 3 nm along with hypochromicity of ~43%. Similar spectral changes are also observed for the dpq and dppz complexes indicating the primarily groove-binding nature of the complexes. The K_b values obtained by this method are 6.2×10^3 for **1**, 1.0×10^4 for **2**, and $5.7 \times 10^4 \text{ M}^{-1}$ for **3** (Figure 3).

(40) (a) Barton, J. K.; Danishefsky, A. T.; Goldberg, J. M. *J. Am. Chem. Soc.* **1984**, *106*, 2172. (b) Kelly, T. M.; Tossi, A. B.; McConnel, D. J.; Strekas, T. C. *Nucleic Acids Res.* **1985**, *13*, 6017. (c) Tysoe, A.; Morgan, R. J.; Baker, A. D.; Strekas, T. C. *J. Phys. Chem.* **1993**, *97*, 1707.



Figure 4. Cleavage of supercoiled pUC19 DNA (33 μM) by $[\text{Cu}(\text{py}_2\text{-phe})\text{B}](\text{ClO}_4)_2$ (B = phen, **1**; dpq, **2**; dppz, **3**; 40 μM) using 3-mercaptopropionic acid (MPA, 5 mM) as a reducing agent in the presence or absence of additives in a 50 mM Tris-HCl/NaCl buffer (pH 7.2) at 37 $^\circ\text{C}$ containing DMF (10%): lane 1, DNA control; lane 2, DNA + **3**; lane 3, DNA + MPA; lanes 4–6, DNA + complexes **1–3**, respectively, + MPA; lane 7, DNA + distamycin (100 μM) + **2** + MPA; lane 8, DNA + distamycin (100 μM) + **3** + MPA; lane 9, DNA + DMSO (2 μL) + **3** + MPA; lane 10, DNA + NaN_3 (100 μM) + **3** + MPA.

Scheme 2. (a) Schematic View Showing the Steric Protection of the Phen Ligand in $[\text{Cu}(\text{py}_2\text{phe})(\text{phen})]^{2+}$ at the Minor Groove of Duplex DNA.^a (b) Mechanistic Pathway Proposed for the DNA Photocleavage Activity of **2** and **3** at 365 nm and for the Chemical Nuclease Activity in the Presence of MPA.



^a phen = dark shade and py_2phe = light shade.

Chemical Nuclease Activity. The chemical nuclease activity of the complexes has been studied using supercoiled (SC) pUC19 DNA in a medium of Tris-HCl/NaCl buffer in the presence of MPA as a reducing agent. The observed DNA cleavage activity order is **3** > **2** \gg **1** (Figure 4). A 40 μM dppz complex completely cleaves SC DNA to its NC form, while its dpq analogue shows \sim 80% cleavage in dark in the presence of MPA. The phen complex is relatively poor cleaver of DNA as the steric encumbrance of the tripodal py_2phe ligand affects the binding of the phen complex to DNA (Scheme 2a). In the presence of the minor groove binder distamycin, the dpq complex shows inhibition of cleavage, while the dppz complex displays no apparent inhibition. The results suggest minor and major groove binding preferences for the dpq and dppz complexes, respectively.³⁸ The presence of a hydroxyl radical scavenger like DMSO inhibits the “chemical nuclease” activity of the complexes. We suggest a cleavage pathway involving the formation of reactive hydroxyl radical or copper-oxo species similar to the one proposed for the “chemical nuclease” activity of the bis-phen copper(I) complex (Scheme 2b).^{41–44}

Table 3. Photoinduced SC pUC19 DNA (0.2 μg , 33 μM) Cleavage Data^a Using **2** and **3** at 365, 632.8, and 694 nm

Sl no.	conditions	[complex] (μM)	λ (nm)	t (min)	% SC	% NC	% linear
1	DNA control	—	365	60	92	8	—
2	DNA + 2	50	365	15	12	88	—
3	DNA + 2	50	365	30	1	90	9
4	DNA + 2	50	365	60	1	46	53
5	DNA + 3	25	365	15	1	99	—
6	DNA + 3	25	365	30	1	80	19
7	DNA + NaN_3 + 2	50	365	15	90	10	—
8	DNA + D_2O + 2	50	365	15	5	55	40
9	DNA + 2 (argon)	50	365	15	92	8	—
10	DNA control	—	632.8	120	98	2	—
11	DNA + 2	100	632.8	120	1	56	43
12	DNA + 3	100	632.8	60	2	53	45
13	DNA control	—	694	120	95	5	—
14	DNA + 2	200	694	120	32	68	—
15	DNA + 3	100	694	120	28	72	—

^a $[\text{NaN}_3]$, 100 μM ; D_2O , 14 μL ; SC, NC, and linear are different forms of DNA.

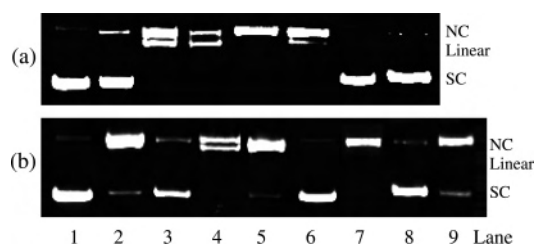


Figure 5. (a) Gel electrophoresis diagram showing the cleavage of SC pUC19 DNA (0.2 μg , 33 μM) by **1–3** using monochromatic UV radiation of 365 nm (12 W) at different complex concentrations and exposure times: lane 1, DNA control (60 min); lane 2, DNA + **1** (50 μM , 60 min); lane 3, DNA + **2** (50 μM , 30 min); lane 4, DNA + **2** (50 μM , 60 min); lane 5, DNA + **3** (25 μM , 15 min); lane 6, DNA + **3** (25 μM , 30 min); lane 7, DNA + **2** (50 μM , in dark, 1 h); lane 8, DNA + **3** (25 μM , in dark, 1 h). (b) Cleavage of SC pUC19 DNA (0.2 μg , 33 μM) by **2** and **3** (50 μM) in the presence of different additives on photo irradiation at 365 nm for 15 min in 50 mM Tris-HCl/NaCl buffer (pH 7.2) containing DMF (10%) under aerobic conditions (except for lane no. 6): lane 1, DNA control; lane 2, DNA + **2**; lane 3, DNA + NaN_3 (100 μM) + **2**; lane 4, DNA + D_2O (14 μL) + **2**; lane 5, DNA + DMSO (2 μL) + **2**; lane 6, DNA + **2** (under argon); lane 7, DNA + **3**; lane 8, DNA + NaN_3 (100 μM) + **3**; lane 9, DNA + DMSO (2 μL) + **3**.

Photoinduced DNA Cleavage. The cleavage activity of the complexes has been studied using plasmid supercoiled pUC19 DNA in a medium of Tris-HCl/NaCl buffer on irradiation with monochromatic UV light of 365 nm and red light of 632.8 and 694 nm. Selected cleavage data are given in Table 3. Complex **1** is a poor cleaver of DNA on exposure to light at 365 nm. A 50 μM solution of the dpq complex, **2**, on irradiation at 365 nm for 30 min, however, shows essentially complete cleavage of SC DNA to its nicked circular (NC) form along with the formation of the linear form of DNA whose quantity increases on increasing the photoexposure time (Figure 5). The dppz complex, **3**, is more reactive as it shows cleavage activity similar to that of **2** but with a much reduced complex concentration and less exposure time. The dppz complex also shows the formation of linear DNA resulting from double-strand breaks. Literature

(43) Zelenko, O.; Gallagher, J.; Sigman, D. S. *Angew. Chem., Int. Ed. Engl.* **1997**, *36*, 2776.

(44) (a) Johnson, G. R. A.; Nazhat, N. B. *J. Am. Chem. Soc.* **1987**, *109*, 1990. (b) Yamamoto, K.; Kawani, S. *J. Biol. Chem.* **1989**, *264*, 15435. (c) Que, B. G.; Downey, K. M.; So, A. G. *Biochemistry* **1980**, *19*, 5987.

(41) Meijler, M. M.; Zelenko, O.; Sigman, D. S. *J. Am. Chem. Soc.* **1997**, *119*, 1135.

(42) Graham, D. R.; Marshall, L. E.; Reich, K. A.; Sigman, D. S. *J. Am. Chem. Soc.* **1980**, *102*, 5419.

reports show that ruthenium(II) polypyridyl complexes containing the dibenzo[h,j]dipyrido[3,2-a:2',3'-c]phenazine ligand display DNA double-strand breaks by singlet oxygen as a result of partial intercalative binding of the complexes to plasmid DNA.⁴⁵ Control experiments with only SC-DNA exposed to 365 nm or the SC-DNA in the presence of dpq or dppz complex in absence of light do not show any significant cleavage of DNA. The photocleavage reactions are studied using different additives. The complexes are cleavage inactive in an argon atmosphere indicating the necessity of molecular oxygen. The DNA cleavage reactions involving $^3\text{O}_2$ could proceed via two major mechanistic pathways.^{8,46} The singlet excited electronic state of the complex, through efficient intersystem crossing, could generate the excited triplet state of the photosensitizer that can activate molecular oxygen from its stable triplet ($^3\text{O}_2$, $^3\Sigma_g^-$) to the reactive singlet ($^1\text{O}_2$, $^1\Delta_g$) state by a type-II process (Scheme 2b). In an alternate pathway, the excited-state complex could reduce molecular oxygen to generate reactive hydroxyl radicals. We have observed that the addition of the singlet oxygen quencher sodium azide to SC-DNA significantly inhibits the photoinduced DNA cleavage activity of the dpq complex at 365 nm. The hydroxyl radical scavenger DMSO has no apparent effect on the cleavage activity. The results suggest the involvement of singlet oxygen in the photocleavage reactions on UV light irradiation. The formation of singlet oxygen is also indicated from the reaction in D_2O showing enhancement of the cleavage activity.⁴⁷ The dpq or dppz ligand alone is cleavage inactive at 365 nm under similar experimental conditions. Control experiments have been carried out using monomeric copper(II) complexes $[\text{Cu}(\text{dpq})(\text{NO}_3)_2(\text{OH}_2)]$ (**I**) and $[\text{Cu}(\text{dppz})(\text{NO}_3)_2(\text{OH}_2)]$ (**II**) in which the photosensitizer base is unprotected from solvent quenching in absence of any sterically encumbered tripodal ligand.⁴⁸ Both **I** and **II** show relatively poor DNA cleavage activity under similar reaction conditions, while copper(II) scorpionates $[\text{Cu}(\text{Tp}^{\text{Ph}})\text{B}]^+$ display significantly higher cleavage activity than **2** and **3** (Figure 6). The steric protection of dpq and dppz as photosensitizer is relatively more in the $\{\text{Cu}(\text{Tp}^{\text{Ph}})\}$ bowl.³⁸

Both the dpq and dppz complexes show photoinduced DNA-cleavage activity at red light of 632.8 nm (low-power CW He–Ne laser, 3 mW) and 694 nm (pulsed ruby laser, 1/6 Hz, 20 ns) (Figure 7). A 100 μM solution of the dppz complex on 1 h exposure at 632.8 nm displays essentially complete cleavage of DNA from its SC to NC (53%) and linear (45%) forms. Significant cleavage of SC DNA to its NC form is observed at 694 nm. A 100 μM solution of the dppz complex **3** on a 2 h exposure at this wavelength gives $\sim 70\%$ cleavage of SC-DNA. The dppz complex consistently

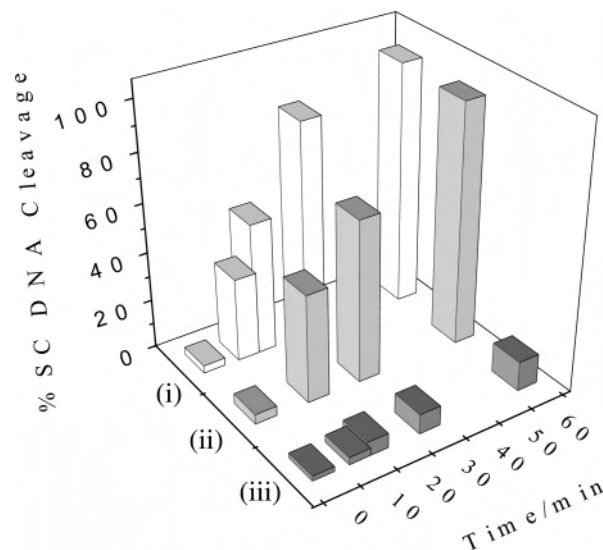


Figure 6. Cleavage of pUC19 DNA (33 μM) by $[\text{Cu}(\text{Tp}^{\text{Ph}})(\text{dpq})](\text{ClO}_4)$ [(i), 25 μM], $[\text{Cu}(\text{py}_2\text{phe})(\text{dppz})](\text{ClO}_4)_2$ (**3**) [(ii), 100 μM], and $[\text{Cu}(\text{dppz})(\text{NO}_3)_2(\text{H}_2\text{O})]$ [(iii), 100 μM] at different photoexposure time using a CW He–Ne laser of 632.8 nm.

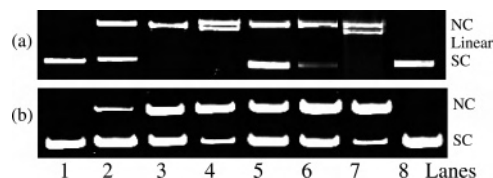


Figure 7. (a) Red light-induced cleavage of SC pUC19 DNA (33 μM) by complexes **2** (100 μM) and **3** (100 μM) in 50 mM Tris-HCl/NaCl buffer (pH 7.2) containing DMF (10%) using a 632.8 nm CW laser (3 mW) at different exposure times: lane 1, DNA control (2 h); lane 2, DNA + **2** (30 min); lane 3, DNA + **2** (1 h); lane 4, DNA + **2** (2 h); lane 5, DNA + **2** (3 h); lane 6, DNA + **3** (45 min); lane 7, DNA + **3** (60 min); lane 8, DNA + **3** (in dark). (b) Gel diagram showing the cleavage of SC DNA (33 μM) by **2** (200 μM) and **3** (100 μM) using a pulsed ruby laser (694 nm, 30 mJ/P peak power): lane 1, DNA control (2 h); lane 2, DNA + **2** (30 min); lane 3, DNA + **2** (1 h); lane 4, DNA + **2** (2 h); lane 5, DNA + **3** (30 min); lane 6, DNA + **3** (1 h); lane 7, DNA + **3** (2 h); lane 8, DNA + **3** (in dark, 2 h).

shows greater DNA cleavage activity than its dpq analogue at all the three wavelengths we have studied.

The “chemical nuclease” and photoinduced DNA cleavage activity of the present complexes and their Tp^{Ph} analogues show interesting trend.^{17,38} Complexes **1–3** display better DNA binding propensity than their Tp^{Ph} analogues because of the lesser steric bulk of the py_2phe ligand, and the present complexes show significantly enhanced “chemical nuclease” activity in the presence of MPA. The steric encumbrance of the $\{\text{Cu}(\text{Tp}^{\text{Ph}})\}$ bowl is more than that of the $\{\text{Cu}(\text{py}_2\text{phe})\}$ unit, and this has a significant effect on the protection of the heterocyclic base like dpq and dppz in its photoexcited state from quenching by the solvent molecules. The photoinduced DNA cleavage activity of $[\text{Cu}(\text{Tp}^{\text{Ph}})\text{B}]^+$ is more than its py_2phe analogue ($\text{B} = \text{dpq}, \text{dppz}$). Control experiments have shown that dpq and dppz ligands alone with their photoexcited $^3(n-\pi^*)$ and $^3(\pi-\pi^*)$ states are unable to cleave DNA at 365 nm (12 W) or at red light. The same ligand when bound to copper(II) exhibits significant DNA cleavage even at red light wavelengths of 694 and 632.8 nm, which is close to the wavelength used for photoactivation of the PDT drug Photofrin. The metal ion thus plays a major

(45) Hergueta-Bravo, A.; Jimenez-Hernandez, M. E.; Montero, F.; Oliveros, E.; Orellana, G. *J. Phys. Chem. B* **2002**, *106*, 4010.

(46) Meunier, B.; Pratiel, G.; Bernadou, J. *Bull. Soc. Chim. Fr.* **1994**, *131*, 933.

(47) Khan, A. U. *J. Phys. Chem.* **1976**, *80*, 2219. (b) Merkel, P. B.; Kearns, D. R. *J. Am. Chem. Soc.* **1972**, *94*, 1029.

(48) Thomas, A. M.; Nethaji, M.; Mahadevan, S.; Chakravarty, A. R. *J. Inorg. Biochem.* **2003**, *94*, 171.

role in the photoexcitation process. Our earlier studies have shown that DNA cleavage by ternary complexes is metal-assisted and involves the metal-based charge transfer and d–d transitions in the photoexcitation process.²⁶ Since the present complexes show a d–d band in the range of 675–701 nm in their electronic spectra, photoexcitation by the ruby laser of 694 nm could involve this band in showing efficient DNA cleavage at this longer wavelength.

Conclusions

Ternary copper(II) complexes in which the DNA binder cum photosensitizer phenanthroline bases, such as dpq and dppz, are in a {Cu(py₂phe)} bowl formed by a tripodal ligand are prepared, and their 1,10-phenanthroline analogue is structurally characterized by X-ray crystallography. The complexes display efficient binding to CT-DNA and chemical nuclease activity in the presence of 3-mercaptopropionic acid as a reducing agent. The dpq and dppz complexes show cleavage of supercoiled DNA on photoexcitation at 365 nm, involving the formation of singlet oxygen as the reactive species. The observation of a low energy d–d band near 700 nm for the dppz complex is of importance as porphyrins including Photofrin are known to show visible bands at relatively shorter wavelengths. The dpq and dppz complexes exhibit visible light-induced DNA cleavage activity at red light of 632.8 and 694 nm with the formation of linear DNA in significant quantity. The observation of efficient photocleavage of DNA at 694 nm using a pulsed ruby laser is of significance in the PDT chemistry as human tissue has greater

transparency at this wavelength than at 630 nm, the wavelength known for photoactivation of the PDT drug Photofrin. The present study shows the positive effect of steric protection of the photosensitizer by the ancillary ligand from solvent quenching of the excited electronic state. The steric effect which is akin to the molecular light switch effect observed for tris-chelates of emissive transition metal complexes, significantly enhances the photoinduced DNA cleavage activity of the ternary copper(II) complexes.

Acknowledgment. We thank the Council of Scientific and Industrial Research, New Delhi, for financial support (CSIR, 01/1841/03/EMR-II), the Department of Science and Technology, Government of India, for the CCD facility and funding (DST/SR/S1/IC-10/2004), Professor P. K. Das of our department and the Chairman of the Chemical Engineering Department for the laser facility, the Alexander von Humboldt Foundation for an electrochemical system, and the Convener Bioinformatics Center of our Institute, for database searching.

Supporting Information Available: Figures S1–S5 showing emission spectral plot, DNA melting plot, cyclic voltammograms of the complexes, gel electrophoresis diagram, and unit cell packing diagram for 1·MeCN, tables listing full crystallographic data, atomic coordinates, bond distances and angles, anisotropic thermal parameters, and hydrogen atom coordinates for the complex 1·MeCN (CIF). This material is available free of charge via the Internet at <http://pubs.acs.org>.

IC0505246